Macromolecules

ARTICLE

pubs.acs.org/Macromolecules

Carbazole-Based Copolymers: Effects of Conjugation Breaks and Steric Hindrance

Jinseck Kim,[†] Young Soo Kwon,[†] Won Suk Shin,[‡] Sang-Jin Moon,[‡] and Taiho Park*[,†]

[†]Department of Chemical Engineering, Polymer Research Institute, Pohang University of Science and Technology, Pohang 790-784, Korea

[‡]Energy Materials Research Center, Korea Research Institute of Chemical Technology (KRICT), 100 Jang-dong, Yuseong-gu, Daejeon 305-600, Korea

Supporting Information

ABSTRACT: A series of carbazole-based D-π-A copolymers were synthesized to investigate the influences of conjugation length and structural distortion on intramolecular charge transfer (CT) complexation between the donor (D) and acceptor (A) components. Carbazole presents two possible linkage sites, the 2,7- and 3,6-positions, which led to significant differences in the thermal, photophysical, electrochemical, and electrical properties of the copolymers due to the positioning of the electron-rich nitrogen atom with respect to the copolymer backbone. The copolymers were comprehensively characterized using TGA, DSC, UV−vis, and photoluminescence spectroscopy, cyclic voltammetry, and DFT calculations. P(3,6C-DTBT), which was linked by a thienyl-2′,1′,3′-benzothiadiazole (DTBT) group at the 3,6-positions of the carbazoles so as to directly involve the electron-rich nitrogen atoms in conjugation, exhibited conjugation breaks in the middle of the carbazole units. The breaks resulted in a robust coplanar structure with an extraordinarily low oxidation potential and the ability to stably generate excitons, in contrast with P(2,7C-DTBT), which was linked by DTBT at the 2,7-positions of the carbazole. Two additional hexyl substituents at the 4-position of the thiophene in the DTBT groups of P(2,7C-HDTBT) and P(3,6C-HDTBT), which were identical to P(2,7C-DTBT) and P(3,6C-DTBT), respectively, except for the presence of the substituents, introduced steric hindrance between the D and A units, thereby breaking the coplanarity. Finally, the hole mobilities of the 3,6-carbazole-based copolymers were 1 order of magnitude higher than those of 2,7-carbazole-based copolymers, measured in hole-only devices. This result indicated the presence of stable radical cations and dications at the nitrogen atoms of the copolymers. This work deepens our understanding of carbazole-based D-π-A copolymers and provides insight into the design of novel materials for optoelectronic devices.

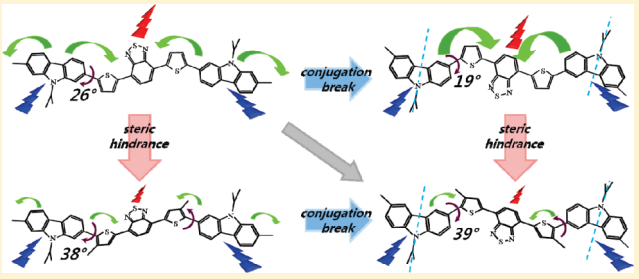

INTRODUCTION

For more than two decades, a variety of polythiophene, polyfluorene, polysilafluorene, polycarbazole, polydithienosilole, and poly(*p*-phenylenevinylene) polymers (and their derivatives) have been actively synthesized for use in organic light-emitting diodes (OLEDs),[1] organic thin film transistors (OTFTs),[2] and organic photovoltaic cells (OPVs).[3] Among these, carbazole-based polymers have received much attention due to their high device performances and many merits, such as the low cost of the starting material (9*H*-carbazole),[4] superior thermal and oxidation stability,[5] high photoconductivity, and propensity to form charge-transfer complexes due to the electron-donating character of the carbazole moiety.[6,7] The advantages of carbazole-based compounds arise from the presence of the nitrogen atom, which carries lone pair electrons.[8] Lone pair electrons not only provide electron-donation capacity to the carbazole units, they activate specific positions for electrophilic aromatic substitution, particularly for producing carbazole derivatives functionalized at the 3,6-position. Recently, alternative synthetic strategies were developed for the easy synthesis of carbazole derivatives functionalized at the 2,7-position.[9] Each link in the carbazole derivative can significantly affect the properties of the resulting polymers. Therefore, understanding the structural differences produced by the choice of position linkage in the carbazole is important and can facilitate the tailored application of carbazole derivatives to a range of specific purposes.[1,4]

The differences between the properties of polymers with 2,7- or 3,6-position carbazole linkers arise from the position of the nitrogen atom. The 2,7-carbazole-based polymers feature conjugation that is entirely over the sp^2-carbons of the main backbone.[10,11] In this case, the nitrogen atom is at the *meta* position in the conjugated framework. In contrast, the nitrogen atom of 3,6-carbazole-based polymers is at the *para* position in the conjugated framework and significantly influences the polymer properties.[12] Differences in the electron-donating properties suggest that the linkage provides a handle for tuning

Received: October 30, 2010
Revised: February 1, 2011
Published: February 28, 2011

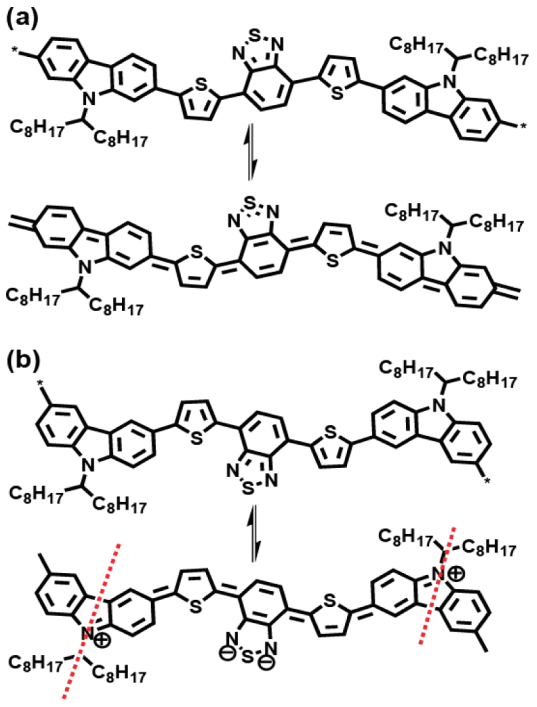

Figure 1. Equilibria between the aromatic structure and the quinoid structure in a copolymer with 2,7-linked carbazole (a) or 3,6-linked carbazole (b) with DTBTs. The dotted line indicates a conjugation break.

intramolecular charge transfer (CT) and, therefore, the electrochemical, optical, and electronic properties of the resulting polymers. Intramolecular CT complexes may be formed using materials with alternating electron-rich carbazole derivatives (electron donor: D) and electron-deficient moieties (electron acceptor: A).[8,13] The copolymer composition allows control over the energy level of the highest occupied molecular orbital (HOMO) and the bandgap between the HOMO and the lowest unoccupied molecular orbital (LUMO). Indeed, 2,7-carbazole-based copolymers with a low bandgap, P(2,7C-DTBT), were synthesized and used as an active material in organic solar cells. The devices exhibited excellent power conversion efficiencies up to 6.1%.[3] A common feature of successful active materials is effective intramolecular CT facilitated by the electron-donating and -accepting D and A units. The coplanarity of the D and A moieties is also important and is assisted by the quinoidal structure of the conjugated polymer backbone (Figure 1a).[14]

The electron-donating strength of the 3,6-carbazole to an electron-deficient unit is stronger than that of the 2,7-carbazole because the nitrogen atom is at the *para* position with respect to the backbone in the 3,6-carbazole derivative. Stronger intramolecular CT is expected in 3,6-carbazole-based copolymers.[15] A more planar conjugated backbone is expected to facilitate chain−chain interactions among the copolymers and improve hole mobility. Materials with these properties are excellent for producing deep blue organic light-emitting diodes[16,17] and electrochromic materials.[18,19] Alternatively, the quinoidal structure may produce a discontinuity in the conjugation at the nitrogen atom, yielding a conjugation break in the polymer backbone (Figure 1b).[15,20,21] There are several examples of 3,6-carbazole-based copolymers formed from comonomers with an electron-deficient state, for example, 2,5-dibromothiophene,[15] 2,2′-dibromo-5,5′-bithiophene,[15] 4,7-dibromo-2,1,3-benzothiadiazole[22] (BT), and 4,7-divinylene-2,1,3-benzothiadiazole.[23] The molecular weights of the copolymers were in the range of 2−5 kDa (M_n) due to low solubility. To improve the molecular weight and solubility of the 3,6-carbazole-based copolymers, bulk comonomers were introduced, such as 1,1-dimethyl-3,4-diphenyl-2,5-bis(4′-bromophenyl)-3,4-diphenylsilole,[24] or alkyl-substituted comonomers, such as 4,4-dibromo-9,9-dioctylfluorene.[25]

Several researchers have described the effects of long alkyl groups in D-π-A copolymers in terms of their electrochemical, optical, and electronic properties. Song et al. synthesized a 2,7-dihydroindeno[2,1-*a*]indene-based copolymer that incorporated DTBT units modified with alkyl substituents at the 4-position of the thienyl units.[26] UV−vis absorption measurements indicated that the alkyl substituents led to severe steric hindrance, which twisted the conjugated backbone between D and A units. The optical bandgap was, then, increased relative to the control copolymer without alkyl substituents on the thienyl units. This result agreed with the results of a computational simulation. In contrast, Zhou et al., who studied a copolymer that was identical except for the substitution of a benzo[2,1-*b*:3,4-*b*′]dithiophene derivative in place of the 2,7-dihydroindeno[2,1-*a*]indene unit as the electron-donating unit, found that alkyl substituents at the 3-position of the DTBT thienyl units significantly influenced the optical properties. The twisted conjugated backbone led to an increase in the optical bandgap. However, minimum steric hindrance was observed in copolymers having alkyl substituents at the 4-positions.[27] Wang et al. prepared a series of fluorene-based copolymers with bis(thiophen-2-yl)benzo[*c*]-1,2,5-thiadiazole (DBT). They introduced alkyl groups at three sites on the thienyl units.[28] Interestingly, the extra alkyl groups served as additional electron-donating substituents, resulting in a smaller bandgap compared to the control copolymer. The HOMO energy levels of the copolymers were comparable to those of the control copolymers. This result indicated that the alkyl substituents did not introduce steric hindrance. Even, Qin et al. synthesized poly(2-(5-(5,6-bis(octyloxy)-4-(thiophen-2-yl)benzo[*c*]-1,2,5-thiadiazol-7-yl)thiophen-2-yl)-9-octyl-9*H*-carbazole), and surprisingly, this polymer showed high crystalline nature with planar backbone in spite of existence of two alkoxy group at 5- and 6-position of BT.[29] The seemingly contradictory results described above may be rationalized in terms of the difference in the electron-donating power, although other factors (e.g. alkyl chain lengths,[30] the presence of branches,[31] the presence of an anchoring position,[27] interactions with an alkyl group of a donor aromatic unit,[27] and the presence of a spacer unit between an electron donor unit and an acceptor unit[28]) may contribute to the overall properties.

In this article, we describe a systematic study of the effective conjugation length of carbazole-based copolymers in view of conjugation breaks and steric hindrance. As shown in Figure 2, a series of carbazole-based copolymers were prepared. Combinations of the fully conjugated 2,7-carbazole and planar DTBT structures were expected to produce a linear alternating copolymer, poly[*N*-9′-heptadecanyl-2,7-carbazole-*alt*-5,5-(4′,7′-di-2-thienyl-2′,1′,3′-benzothiadiazole)] P(2,7C-DTBT),[32] in which formation of an intramolecular CT complex was favored. Poly[*N*-9′-heptadecanyl-3,6-carbazole-*alt*-5,5-(4′,7′-di-4-hexyl-2-thienyl-2′,1′,3′-benzothiadiazole)], P(3,6C-DTBT), was synthesized, which featured a more robust coplanarity between the D and A units, probably due to the strong electron-donating nature of the

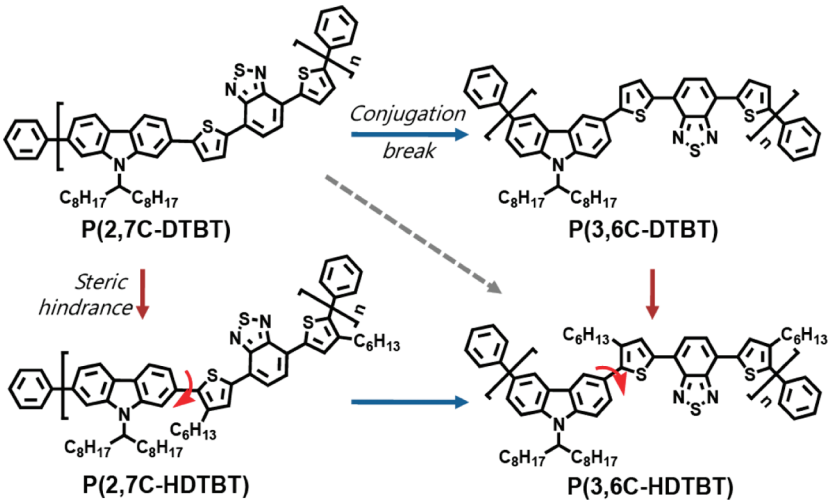

Figure 2. Schematic diagram of the potential causes of conjugation breaks, steric hindrance, or both, in each of the four copolymers.

nitrogen atom and the resulting preference for a quinoid structure. In addition, the effects of steric hindrance, due to the alkyl substituents, on the dihedral angles and coplanarity of the backbone were investigated using alkyl-substituted DTBT-incorporated copolymers, poly[*N*-9′-heptadecanyl-2,7-carbazole-*alt*-5,5-(4′,7′-di-4-hexyl-2-thienyl-2′,1′,3′-benzothiadiazole)], P(2,7C-HDTBT), and poly[*N*-9′-heptadecanyl-3,6-carbazole-*alt*-5,5-(4′,7′-di-4-hexyl-2-thienyl-2′,1′,3′-benzothiadiazole)], P(3,6C-HDTBT).

EXPERIMENTAL SECTION

Materials and Characterization. 2,7-Bis(4′,4′,5′,5′-tetramethyl-1′,3′,2′-dioxaborolan-2′-yl)-*N*-9′′-heptadecanylcarbazole (2,7-carbazole), 4,7-bis(5-bromo-2-thienyl)-2,1,3-benzothiadiazole (DTBT), and 4,7-bis(5-bromo-4-hexyl-2-thienyl)-2,1,3-benzothiadiazole (HDTBT) were synthesized according to the previously reported procedures.[9,32−34] Tetrahydrofuran (THF) was purified using a J. C. Meyer solvent dispensing system. All other chemicals were purchased from Sigma-Aldrich Co. and Junsei Co. and used without purification.

^{1}H and ^{13}C NMR spectra were recorded on a Bruker DPX-300 (300 MHz) FT-NMR system operated at 300 and 75 MHz, respectively. ^{1}H and ^{13}C NMR spectra of P(2,7C-DTBT) and P(3,6C-DTBT) were recorded on a Bruker DRX-500 FT-NMR system operated at 130 °C, at 500 and 75 MHz, respectively. Elemental analyses were performed by Organic Chemistry Research Center (elemental analyzer; CE Instruments Flash EA 1112 series). High-resolution mass spectra were obtained from the Deagu Branch Analytical Laboratory of the Korea Basic Science Institute (high-resolution mass spectrometer, JEOL JMS 700 model). Thermogravimetric analysis (TGA) and differential scanning calorimetric (DSC) measurements of the copolymers were performed using a Perkin-Elmer Pyris 1 TGA instrument and a Seiko DSC 220 CU instrument under a nitrogen atmosphere at a heating and cooling rate of 10 °C/min. Number-average (M_n) and weight-average (M_w) molecular weights were determined by gel permeation chromatography (GPC) using the Shimadzu LC solution, chloroform as the eluent, and a calibration curve of polystyrene standards. The UV−vis absorption spectra were measured using a Carry 5000 UV−vis−near-IR double-beam spectrophotometer, and photoluminescence (PL) spectra of the copolymers were measured on a Jasco FP-6500 spectrometer. Cyclic voltammetry was performed using a PowerLab/AD instrument model system in a three-electrode cell with a 0.1 M Bu_4NBF_4 solution in acetonitrile at a scan rate of 50 mV s^{-1}. A glassy carbon disk (~0.05 cm^2) coated with a thin polymer film was used as the working electrode. A platinum wire and an $Ag/AgNO_3$ electrode were used as the counter and reference electrodes, respectively.

Space Charge Limited Current (SCLC) Measurements. Hole-only devices were fabricated on top of a prepatterned ITO substrate. After cleaning the ITO with aqueous detergent, deionized water, acetone, and 2-propanol, UV-ozone treatment was applied for 15 min. PEDOT:PSS (Baytron P TP AI 4083, Bayer AG) was spin-coated from an aqueous dispersion phase to a layer 36 nm thick. The coated substrate was then baked at 120 °C for 60 min. After baking, a solution of the copolymer in chloroform was spin-cast on top of the PEDOT:PSS layer to a thickness of ~50 nm, and the samples were dried for 6 h at room temperature under vacuum conditions. The Pd electrode was deposited by thermal evaporation under a vacuum of ~10^{-6} Torr.

Synthesis of the Monomers and Carbazole-Based Copolymers. *N-9′-Heptadecanyl-3,6-dibromocarbazole (**2**).* 3,6-Dibromo-9*H*-carbazole (4.00 g, 12.3 mmol) and potassium hydroxide (6.90 g, 123 mmol) were dissolved in 30 mL of dried dimethyl sulfoxide (DMSO), and the mixture was stirred for 1 h. To this solution were added a catalytic amount of 18-crown-6 dissolved in 5 mL of DMSO and a 9-heptadecane *p*-toluenesulfonate (7.58 g, 18.45 mmol) solution dissolved in 15 mL of DMSO, dropwise, and the solution was stirred overnight.

The solution was poured into water and extracted three times with hexane/ethyl acetate (3:1 v/v). The organic layer was washed with distilled water and dried over $MgSO_4$. Solvent was removed by rotary evaporation, and the remaining yellow liquid was purified by silica gel column chromatography with hexane to give a white solid (6.01 g, yield: 86%). ^{1}H NMR (300 MHz, $CDCl_3$, ppm): δ 8.16 (br, 2H); 7.48 (br, 4H); 4.47 (br, 1H); 2.23 (br, 2H); 1.90 (br, 2H); 1.11 (br, 24H); 0.83 (t, J = 7.1 Hz, 6H). ^{13}C NMR (75 MHz, $CDCl_3$, ppm): δ 129.39; 128.93; 123.73; 123.40; 113.42; 110.94; 57.23; 34.03; 32.13; 29.68; 29.66; 29.50; 27.02; 22.99; 14.47; mp 53.6−55.7 °C. HRMS (EI+, m/z) [M]+ calcd for $C_{29}H_{41}Br_2N$ 561.1606, found 561.1608. Elemental analysis calcd (%) for $C_{29}H_{41}Br_2N$: C 61.82, H 7.33, N 2.49; found: C 61.85, H 7.48, N 2.40.

3,6-Bis(4′,4′,5′,5′-tetramethyl-1′,3′,2′-dioxaborolan-2′-yl)-N-9′′-heptadecanylcarbazole (3,6-Carbazole). *n*-Butyllithium (17.5 mL, 1.7 M solution in hexane, 29.8 mmol) was added dropwise to a solution of compound **2** (4.00 g, 7.1 mmol) in dry THF (30 mL) at −78 °C under nitrogen. The reaction was stirred for 1 h at −78 °C, and 2-isopropoxy-4,4,5,5-tetramethyl-1,3,2-dioxaborolane (5.92 mL, 5.28 g, 28.4 mmol) was added in one portion. The temperature of the solution was increased to room temperature, and the solution was stirred overnight.

Scheme 1. Synthetic Schemes for the Monomers (3,6-Carbazole) and Copolymers (P(2,7C-DTBT), P(3,6C-DTBT), P(2,7C-HDTBT), P(3,6C-HDTBT))[a]

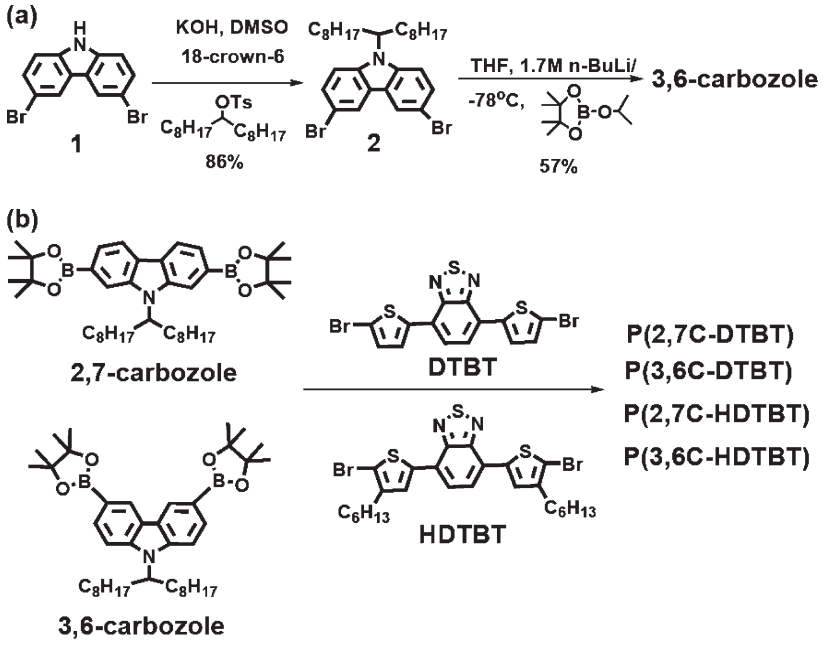

[a] Polymerization conditions: Et_4NOH, $Pd(PPh_3)_4$, toluene, 48 h, 85 °C.

The reaction was quenched by adding distilled water, followed by extraction three times with ether. The organic layer was washed with distilled water and dried over $MgSO_4$. The solvent was removed by rotary evaporation. The residue was purified by silica gel column chromatography (ethyl acetate/hexane 1:15 v/v) and recrystallized with methanol/acetone (10:1 v/v) to give a pure white solid (2.60 g, yield: 57%). ^{1}H NMR (300 MHz, $CDCl_3$, ppm): δ 8.68 (br, 2H); 7.87 (br, 2H); 7.56 (br, 1H); 7.39 (br, 1H); 4.58 (br, 1H); 2.29 (br, 2H); 1.90 (br, 2H); 1.39 (br, 24H); 1.13 (br, 24H); 0.81 (t, J = 6.8 Hz, 6H). ^{13}C NMR (75 MHz, $CDCl_3$, ppm): δ 144.61; 141.20; 132.08; 128.40; 124.25; 122.85; 111.39; 108.66; 83.90; 56.94; 34.10; 32.14; 29.68; 27.10; 25.36; 22.99; 14.47. mp 147.8−149.2 °C. HRMS (EI+, m/z) [M]+ calcd for $C_{41}H_{65}B_2NO_4$ 567.5100, found 567.5103. Elemental analysis calcd (%) for $C_{41}H_{65}B_2NO_4$: C 74.89, H 9.96, N 2.13; found: C 74.74, H 10.06, N 2.09.

P(2,7C-DTBT). To a 25 mL two-neck flask containing 2,7-bis-(4′,4′,5′,5′-tetramethyl-1′,3′,2′-dioxaborolan-2′-yl)-*N*-9′′-heptadecanyl-carbazole (200 mg, 0.304 mmol) and 4,7-di(2′-bromothien-5′-yl)-2,1,3-benzothiadiazole (139 mg, 0.304 mmol) in a mixture of degassed toluene (10 mL) and tetraethylammonium hydroxide 20% solution in water (3 mL) was added a catalyst of tetrakis(triphenyl-phosphine)palladium(0) (5 mg) and four drops of Aliquat 336. The mixture was allowed to stir for 48 h at 85 °C under a nitrogen atmosphere. At the completion of polymerization, the polymer was end-capped with phenylboronic acid (10 mg) and bromobenzene (1 mL). The reaction was poured into methanol (200 mL), and the precipitated solid was recovered by filtration and washed by Soxhlet extraction with acetone, hexane, and chloroform. The chloroform fraction was filtered using Florisil, concentrated under reduced pressure to 5 mL of the polymer solution, reprecipitated into methanol, collected by filtration, and dried under vacuum. The dark violet polymer was obtained (148 mg, 69.1%). ^{1}H NMR (500 MHz, 130 °C, ODCB-d_4, ppm): δ 8.11 (d, J = 3.5 Hz, 2H); 8.02 (d, J = 8.0 Hz, 2H); 7.94 (br, 2H); 7.75 (br, 2H); 7.56 (d, J = 8.0 Hz, 2H); 7.45 (d, J = 4.0 Hz, 2H); 4.73 (br, 1H); 2.42 (br, 2H); 2.05 (br, 2H); 1.23 (br, 8H); 1.22 (br, 16H); 0.71 (t, J = 6.5 Hz, 6H). ^{13}C NMR (125 MHz, 130 °C, ODCB-d_4, ppm): δ 152.96; 147.37; 142.12; 138.98; 129.14; 126.49; 126.22; 125.22; 124.18; 123.49; 120.74; 118.15; 107.84; 57.14; 34.27; 31.69; 29.42; 29.33; 29.07; 27.03; 22.43; 13.60.

P(3,6C-DTBT). Following the procedure described above, 3,6-bis-(4′,4′,5′,5′-tetramethyl-1′,3′,2′-dioxaborolan-2′-yl)-*N*-9′′-heptadecanyl-carbazole (200 mg, 0.304 mmol) and 4,7-di(2′-bromothien-5′-yl)-2,1,3-benzothiadiazole (139 mg, 0.304 mmol) afforded the title copolymer as a dark violet solid (95.2 mg, 44.4%). ^{1}H NMR (500 MHz, 130 °C, ODCB-d_4, ppm): δ 8.53−7.01 (m, 12H); 4.58 (br, 1H); 2.31 (br, 2H); 2.00 (br, 2H); 1.18 (br, 24H); 0.77 (m, 6H). ^{13}C NMR (125 MHz, 130 °C, ODCB-d_4, ppm): δ 153.29; 146.71; 141.29; 138.28; 129.86; 129.77; 129.43; 126.77; 126.27; 125.31; 124.54; 118.14; 111.06; 57.60; 34.51; 32.00; 29.67; 29.50; 29.38; 27.37; 22.73; 13.93.

P(2,7C-HDTBT). Following the procedure described above, 2,7-bis-(4′,4′,5′,5′-tetramethyl-1′,3′,2′-dioxaborolan-2′-yl)-*N*-9′′-heptadecanyl-carbazole (200 mg, 0.304 mmol) and 4,7-bis(5-bromo-4-hexyl-2-thienyl)-2,1,3-benzothiadiazole (191 mg, 0.304 mmol) afforded the title copolymer as a dark red solid (199 mg, 74.8%). ^{1}H NMR (300 MHz, $CDCl_3$, ppm): δ 8.13 (br, 4H); 7.93 (br, 2H); 7.75 (br, 1H); 7.58 (br, 1H); 7.45 (br, 2H); 4.64 (br, 1H); 2.88 (br, 4H); 2.38 (br, 2H); 2.00 (br, 2H); 1.79 (br, 4H); 1.31 (br, 12H); 1.17 (br, 24H); 0.88 (t, J = 6.7 Hz, 6H), 0.81 (t, J = 6.4 Hz, 6H). ^{13}C NMR (500 MHz, $CDCl_3$, ppm): δ 152.86; 142.07; 141.01; 139.74; 137.35; 131.61; 130.56; 125.91; 125.30; 121.82; 120.64; 112.21; 109.65; 56.77; 33.95; 31.74; 31.14; 29.44; 29.35; 29.28; 29.14; 26.98; 22.60; 22.54; 13.97; 13.92.

P(3,6C-HDTBT). Following the procedure described above, 3,6-bis-(4′,4′,5′,5′-tetramethyl-1′,3′,2′-dioxaborolan-2′-yl)-*N*-9′′-heptadecanyl-carbazole (200 mg, 0.304 mmol) and 4,7-bis(5-bromo-4-hexyl-2-thienyl)-2,1,3-benzothiadiazole (191 mg, 0.304 mmol) afforded the title copolymer as a dark red solid (178 mg, 67.3%). ^{1}H NMR (300 MHz, $CDCl_3$, ppm): δ 8.28 (br, 2H); 8.09 (br, 2H); 7.89 (br, 2H); 7.62 (br, 3H); 7.48 (br, 1H); 4.60 (br, 1H); 2.84 (br, 4H); 2.33 (br, 2H); 1.98 (br, 2H); 1.77 (br, 2H); 1.28 (br, 12H); 1.17 (br, 24H); 0.83 (br, 12H). ^{13}C NMR (500 MHz, $CDCl_3$, ppm): δ 152.87; 141.36; 140.77; 139.92; 136.86; 131.85; 130.24; 125.86; 125.30; 125.12; 121.08; 113.56; 110.21;

Table 1. Polymerization Results and Physical Properties of the Copolymers

copolymers	M_n (g/mol)[a]	M_w (g/mol)[b]	PDI[c]	T_d (°C)[d]	T_g (°C)[e]
P(2,7C-DTBT)	21 000	38 500	1.83	432	126
P(3,6C-DTBT)	4 500	6 100	1.36	455	161
P(2,7C-HDTBT)	30 600	55 500	1.81	416	77
P(3,6C-HDTBT)	29 100	42 200	1.45	462	81

[a] Number-average molecular weight determined by GPC in chloroform using polystyrene standards. [b] Weight-average molecular weight. [c] Polydispersity index. [d] Thermal decomposition temperature (with 5 wt % weight loss). [e] Glass transition temperature (the second scan at heating and cooling rates of 10 °C/min).

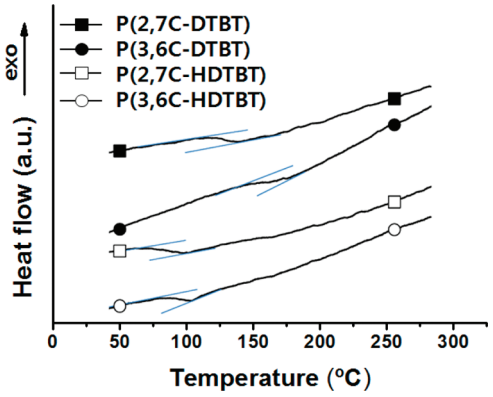

Figure 3. DSC thermograms of P(2,7C-DTBT) (■), P(3,6C-DTBT) (●), P(2,7C-HDTBT (□), and P(3,6C-HDTBT) (○).

56.82; 33.85; 31.70; 31.64; 30.98; 29.34; 29.25; 29.17; 29.08; 29.00; 26.86; 22.54; 13.90.

■ RESULTS AND DISCUSSION

Copolymer Synthesis and Physical Properties. 3,6-Carbazole was synthesized from 3,6-dibromo-9*H*-carbazole, **1**, with a 49% overall yield (two steps) using a modified literature procedure,[22,35] as outlined in Scheme 1. Alkylation of the nitrogen atom in **1** by KOH and 9-heptadecane *p*-toluenesulfonate led to *N*-9′-heptadecanyl-3,6-dibromocarbazole, **2**, in an 86% yield. Lithiation of **2** with *n*-BuLi in THF at −78 °C, followed by quenching with 2-isopropoxy-4,4,5,5-tetramethyl-1,3,2-dioxaborolane, afforded 3,6-carbazole in a 57% yield.

The copolymers described here were prepared by a Suzuki cross-coupling polymerization method. Among the various palladium catalytic systems described elsewhere,[36] $Pd(PPh_3)_4$, with Et_4NOH as a base, exhibited reasonable reproducibility in the polymerization reactions. The copolymerization of 2,7-carbazole with DTBT[33] was carried out for 48 h under a nitrogen atmosphere at 85 °C and then quenched by consecutive additions of phenylboronic acid and bromobenzene to introduce an end-cap into the growing copolymer chains. The crude polymer was then precipitated in methanol and extracted via a Soxhlet apparatus with acetone, hexane, and finally chloroform. Only the chloroform-soluble fraction was collected and filtered, using Florisil, to obtain a solution-processable copolymer with high purity. The resulting purified polymer showed partial solubility in hot chloroform or chlorinated benzene solvents. ^1H NMR spectra of this polymer were measured in *o*-dichlorobenzene (ODCB) at high temperature (130 °C). The molecular weight of P(2,7C-DTBT) measured by GPC was reasonably high (M_n = 21.0 kg/mol), as summarized in Table 1. The monomer with hexyl substituents on the thiophenes, HDTBT,[34] produced a copolymer with a slightly higher molecular weight, P(2,7C-HDTBT), with good solubility in common organic solvents, such as chlorobenzene, THF, toluene, and chloroform. Both of the copolymers P(2,7C-DTBT) and P(2,7C-HDTBT) were amorphous with glass transition temperatures of 126 and 77 °C, respectively (Figure 3).[37]

Copolymerization of 3,6-carbazole and DTBT produced a copolymer with properties that differed significantly from those of P(2,7C-DTBT). The product easily fouled the inside of the reaction flask, resulting in a low molecular weight (M_n = 4.5 kg/mol), similar to results reported in the literature.[15,38−40] This behavior was possibly due to the poor solubility of P(3,6C-DTBT). Indeed, solubilizing the alkyl substituent in HDTBT significantly increased the molecular weight of the copolymer P(3,6C-HDTBT) up to 29.1 kg/mol (M_n), and the resulting polymers exhibited good solubility in common organic solvents, such as THF, chloroform, toluene, or chlorinated benzene.

The glass transition temperature of P(3,6C-DTBT) was 161 °C, 35 °C higher than that of P(2,7C-DTBT), despite the low molecular weight. These results were probably ascribed to conjugation breaks generated in the centers of the 3,6-carbazole units in P(3,6C-DTBT), which led to a rigid planar structure without extended conjugation, as shown in Figure 1.[15,20] The dramatic increase in the molecular weight of P(3,6C-HDTBT) was preliminarily ascribed to the distortion of the coplanarity between the carbazole and thiophene units in the copolymers, caused by the hexyl substituents at the 4-postions of the HDTBT thiophenes.

All copolymers exhibited remarkable thermal stability up to 420 °C, as revealed by TGA (Supporting Information, Figure S1). The degradation and weight losses of the copolymers beyond their thermal decomposition temperature at the first stabilized stage were ca. 41% and 34% for HDTBT- and DTBT-based copolymers, respectively, proportional to the mass of their alkyl substituents. These results indicated that the thermally unstable part of the structure was the junction of the aliphatic alkyl substituents rather than the main aromatic backbone.[6]

Electronic Properties. UV−vis absorption spectra in various solvents (toluene, chlorobenzene, THF, and chloroform) and in thin films were collected to investigate the effects of the nitrogen position with respect to the conjugated connectivity and the steric hindrance of the hexyl substituents (Table 2). Figure 4 shows representative absorption spectra of the copolymers recorded in chloroform. These copolymers did not display any distinctive solvatochromism effects. The absorption peaks at higher energies of around 350 nm were due to the carbazole moiety, as described.[38,41,42] The absorption peaks in the low-energy region, around 550 nm, were identified by comparison to the absorption peaks of thienyl benzothiadiazoles, which appeared at 450 nm (Supporting Information, Figure S3). Therefore, we could assign the absorption peaks at 550 nm to a transition from the intramolecular CT state to the excited state.[43−45]

A comparison of P(2,7C-DTBT) with P(3,6C-DTBT) revealed the structural differences, with respect to optical properties, caused by the position of the conjugation connection between carbazoles and thienylbenzothiadiazole units. In particular, the effective formation of intramolecular CT complexes

Table 2. UV−Vis Absorption Data for Copolymers in Chloroform and in Films

	solution ($CHCl_3$)					film		
copolymer	$A_{max,1}$ (nm)[a]	ε ($A_{max,1}$)[b]	$A_{max,2}$ (nm)[c]	ε ($A_{max,2}$)[d]	A_{edge} (nm)[e]	$A_{max,2}$ (nm)[f]	A_{edge} (nm)[g]	ΔE_0 (eV)[h]
P(2,7C-DTBT)	396	30 556	557	34 429	645	579	660	1.88
P(3,6C-DTBT)	361	37 792	537	22 154	649	551	671	1.85
P(2,7C-HDTBT)	366	40 151	513	31 575	590	533	616	2.01
P(3,6C-HDTBT)	337	40 545	510	25 518	597	528	620	2.00

[a] Maximum absorption wavelengths in the short wavelength region in solution. [b] Absorption coefficient at $A_{max,1}$ in solution. [c] Maximum absorption wavelength of the long wavelength region in solution. [d] Absorption coefficient at $A_{max,2}$ in solution. [e] Absorption edge of a long wavelength region in solution. [f] Maximum absorption wavelength of a long wavelength region in films. [g] Absorption edge of the long wavelengths in films. [h] Optical bandgaps estimated by the onset point of the absorption edge in a film.

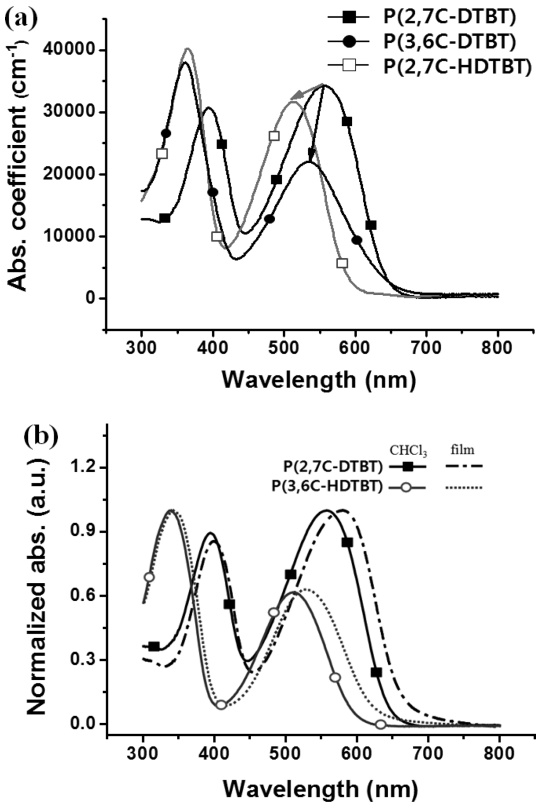

Figure 4. (a) Representative UV−vis spectra of P(2,7C-DTBT) (■), P(3,6C-DTBT) (●), and P(2,7C-HDTBT) (□) in chloroform at room temperature. (b) Comparison of normalized UV−vis spectra of P(2,7C-DTBT) in chloroform (■) and in a film (— · —) and P(3,6C-HDTBT) in chloroform (○) and in a film (· · ·).

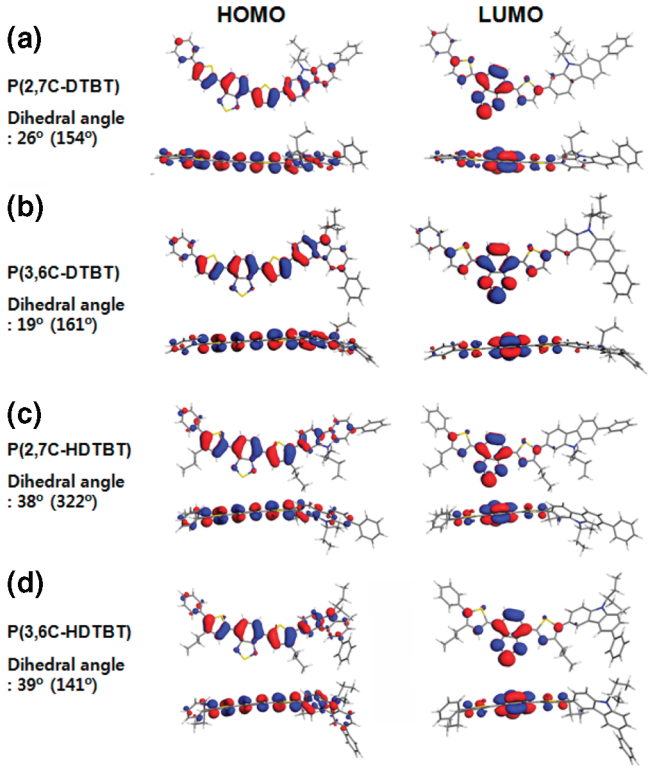

Figure 5. Optimized geometry, electron density distributions of HOMO (left) and LUMO (right), and dihedral angle between carbazole and thienylbenzothiadiazole unit of P(2,7C-DTBT) (a), P(3,6C-DTBT) (b), P(2,7C-HDTBT) (c), and P(3,6C-HDTBT) (d).

was apparent. As shown in Figure 4a, the values of A_{edge} (absorption edges) for P(2,7C-DTBT) and P(3,6C-DTBT) were very similar, 645 and 649 nm, respectively, indicating that effective intramolecular CT occurred from the nitrogen atom of the carbazole unit to the thienylbenzothiadiazole unit in both copolymers to form a quinoidal electronic conformation. However, the absorption maximum (A_{max}) of P(3,6C-DTBT) was slightly blue-shifted relative to that of P(2,7C-DTBT) in chloroform. The values of A_{max} for P(3,6C-DTBT) in chloroform were 361 and 537 nm, which were 35 and 20 nm shorter than the corresponding peaks of P(2,7C-DTBT). Furthermore, the intensity of P(3,6C-DTBT) was stronger at 362 nm due to the carbazole unit but weaker at 537 nm than the corresponding intensities of P(2,7C-DTBT). These results suggested that the effective conjugation lengths might be different in the two copolymers. The conjugation breaks are related to discontinuities in the π-orbital overlap between repeating units of the copolymer and result in shorter effective conjugation lengths. In the case of P(3,6C-DTBT), the effective conjugation length was equivalent to the distance between two nitrogen atoms. In contrast, intramolecular CT was strong in P(2,7C-DTBT), which formed quinoidal electronic conformations through π-orbital overlap with the sp^2-carbons of the main backbone, resulting in a longer conjugation length.[38]

The absorption peaks of the copolymers in thin films were substantially red-shifted and somewhat broadened in comparison with the spectra in chloroform (Figure 4b), indicating increased intermolecular interactions, such as π-stacking.[45] However, no great differences between the substituted (ca. 22 nm in length for P(2,7C-DTBT)) and unsubstituted

Table 3. Electrochemical and Electric Properties of the Copolymers

	$E_{ox,onset}$ (V)[a]	HOMO (eV)[b]	$E_{red,onset}$ (V)[c]	LUMO (eV)[d]	$E_{e,film}$ (eV)[e]	ΔE_0 (eV)[f]	η ($cm^2\ V^{-1}\ s^{-1}$)[g]
P(2,7C-DTBT)	1.10	−5.45	−0.79	−3.56	1.89	1.88	3.2×10^{-6}
P(3,6C-DTBT)	0.83	−5.18	−0.88	−3.47	1.71	1.85	1.2×10^{-5}
P(2,7C-HDTBT)	1.28	−5.63	−0.84	−3.51	2.12	2.01	3.0×10^{-6}
P(3,6C-HDTBT)	1.31	−5.66	−0.85	−3.50	2.16	2.00	1.2×10^{-5}

[a] Onset potential in an anodic scan of the polymers. [b] HOMO levels of the polymers were estimated from E_{onset} of the first oxidation potential relative to ferrocene (F_c), the ionization potential (IP) value of which was −4.8 eV for the F_c/F_c^+ redox system. [c] Onset potential in a cathodic scan of the polymers. [d] LUMO levels of the polymers were estimated from E_{onset} of the first reduction potential relative to ferrocene (F_c), the ionization potential (IP) value of which was −4.8 eV for the F_c/F_c^+ redox system. [e] Electrochemical bandgap determined by the difference between $E_{oxi/onset}$ and $E_{red/onset}$. [f] Optical bandgap was estimated from the absorption edge in the absorption spectra in films. [g] Space charge limited current mobility measured in hole-only devices.

(ca. 18 nm in length for P(3,6C-HDTBT)) copolymers were observed. The substituted polymer displayed a severe dihedral angle, which resulted in inefficient intramolecular charge transfer, and the severe dihedral angle of the substituted polymers was expected to be fairly relaxed in the solid state. A stronger red shift would be expected in the substituted copolymer than in the unsubstituted copolymer. However, the unsubstituted (ca. 22 nm in length for P(2,7C-DTBT)) and substituted (ca. 20 nm in length for P(2,7C-HDTBT)) copolymers did not display significant differences. This result suggested that, even in thin films, the substituted P(3,6C-HDTBT) adopted extensively twisted dihedral angles between the 2,7-carbazole and the HDTBT units due to steric hindrance.

Computational Study. A computational study of the copolymers was performed to deepen our understanding of the observed differences in optical properties. The electronic structures of one repeating units of each copolymer were modeled using density functional theory (DFT) and the Gaussian 03 package at the B3LYP/6-311+G* level of theory.[46,47] The optimized geometry, electron density distributions in the HOMO and LUMO, and the dihedral angle between the carbazole and thienylbenzothiadiazole units are shown in Figure 5 (see Figure S7 and Table S1 for the energy map and detailed energy depending on the dihedral angles, respectively). To simplify the calculations, heptadecanyl and hexyl side chains on the carbazole and thiophenes were replaced with ethylpropyl and propyl groups, respectively. The dihedral angle between the two thienyl groups with a central BT was 5°, in agreement with the value reported in the literature.[27] Therefore, we only focused on the dihedral angle between the thienyl group and the carbazole unit to investigate the effects of steric hindrance due to the hexyl substituents on the thienyl group. The dihedral angle was influenced by the stability of the quinoid structure as well as by the instabilities caused by torsional strain between the fused aromatic units. Thus, as the torsional strain increased or the population of the quinoid structure decreased, the dihedral angle increased (vide infra).

The dihedral angle of P(2,7C-DTBT) was found to be 26°, which was fairly small and indicative of conjugation through π-orbitals on the sp^2-carbons of the main backbone (Figure 5a). The electron density was well-delocalized along the conjugated backbone, as revealed by the isosurface of the HOMO (Figure S6a). Meanwhile, the dihedral angle of P(3,6C-DTBT) was dramatically decreased to 19° (Figure 5b), and the isosurface of the HOMO exhibited delocalized electron density over the regions between two the nitrogen atoms of the two carbazole units, that is, the conjugation break (Figure S6b). These results support the formation of a strong intramolecular CT complex in the ground state, consistent with the observed optical properties.

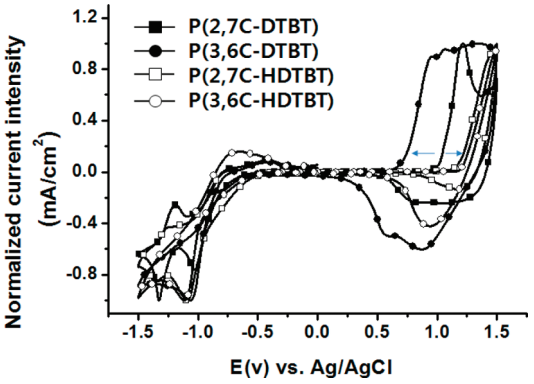

Figure 6. Cyclic voltammograms of P(2,7C-DTBT) (■), P(3,6C-DTBT) (●), P(2,7C-HDTBT (□), and P(3,6C-HDTBT) (○).

Steric hindrance of the hexyl substituents on the HDTBT thiophenes of the copolymers may have decreased the population of the quinoidal electronic configuration in P(2,7C-HDTBT). Steric effects, therefore, could weaken intramolecular CT from the carbazole unit to HDTBT. Indeed, the introduction of alkyl substituents at the 4-position of the thienyl on the DTBT unit greatly influenced the optical properties. The dihedral angles between the 4-substituted HDTBT and the 2- and 7-position or 3- and 6-position linked carbazoles in P(2,7C-HDTBT) and P(3,6C-HDTBT) were 38° and 39°, respectively. Steric hindrance from the extra alkyl substituents at the 4-position on the DTBT unit partially destroyed the quinoidal electronic conformation. This not only reduced formation of an intramolecular CT complex but also shortened the effective conjugation length. Minimization of steric hindrance in the copolymer is tremendously important for achieving materials with strong absorption bands at longer wavelengths. The importance of steric hindrance was also evident in P(3,6C-HDTBT). A_{max} at higher wavelengths was 510 nm, similar to that (513 nm) of P(2,7C-HDTBT). A 39° angle was calculated for the dihedral angle between the 4-substituted HDTBT and the 3- and 6-position linked carbazoles in P(3,6C-HDTBT) (Figure 5d). The severe steric hindrance broke the conjugation at the linkages, reducing the effectiveness of intramolecular CT.

Electrochemical Properties. The electrochemical properties of the copolymers were characterized by cyclic voltammetry (CV) to probe the redox effects of conjugation and alkyl substituent position on the energy levels of the copolymers. The HOMO and LUMO energy levels were determined from

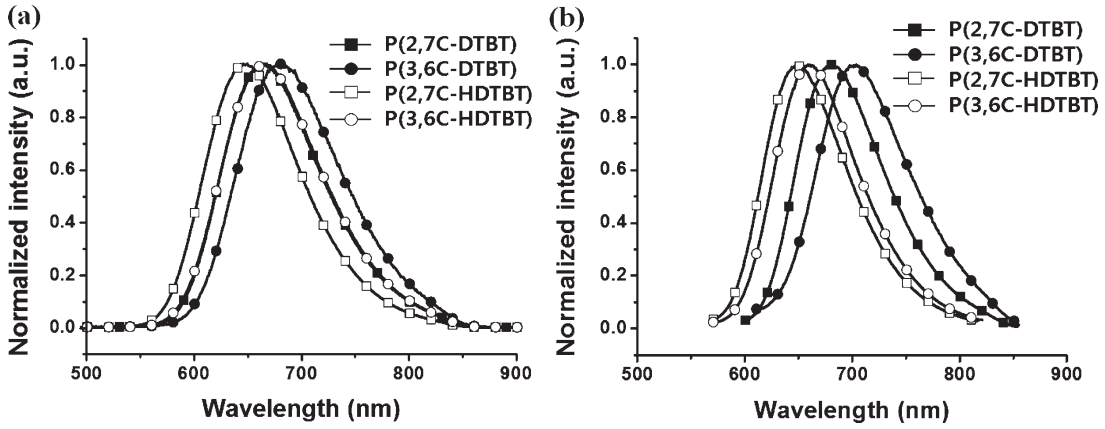

Figure 7. Normalized photoluminescence (PL) spectra of P(2,7C-DTBT) (■), P(3,6C-DTBT) (●), P(2,7C-HDTBT) (□), and P(3,6C-HDTBT) (○) in chloroform (a) and in the film (b). The absorption maxima in short wavelength region, for each sample, were chosen for excitation.

the oxidation and reduction potentials of the copolymers, respectively, relative to ferrocene as an internal standard (the ionization potential of the ferrocene/ferrocenium (Fc/Fc^+) redox system was −4.8 eV).[48] The results are summarized in Table 3.

In the anodic scan, polymers showed onset potentials of 1.10, 0.83, 1.28, and 1.31 V for P(2,7C-DTBT), P(3,6C-DTBT), P(2,7C-HDTBT), and P(3,6C-HDTBT), respectively, against an Ag/AgCl reference electrode (Figure 6). Interestingly, continuous electron transfer reactions were observed in P(3,6C-DTBT) due to radical transfer between the adjacent hetercyclic fused rings. As a result, the copolymers formed an interconnected structure, consistent with previous reports in the literature.[49,50] To achieve a lower oxidation potential in such extensively conjugated copolymers, the electron density on one unit must be high and the oxidized cation must be easily stabilized by the adjacent electron-rich groups. There are three candidate oxidized units in the copolymers: carbazole, thienyl, and benzothiadiazole. The highest electron density would be present in the most electron-richest group, in this case the nitrogen atom, as predicted by the computational study. Therefore, the position of the nitrogen atom, its orientation with respect to the adjacent electron-rich groups, and the dihedral angel between the units containing the nitrogen atom and the adjacent electron-rich groups may be important for estimating the oxidation behavior of the copolymers. Indeed, P(3,6C-DTBT) (in which a nitrogen atom was located at the *p*-positions with respect to the two adjacent thienyl groups and which yielded the smallest dihedral angle (21.7°)) exhibited the lowest onset potential (0.83 V), as summarized in Table 3. The two thienyl groups apparently acted as electron-donating groups in the electrochemical oxidation reactions. The highest onset potential (1.31 V) was obtained in P(3,6C-HDTBT), which had the largest dihedral angle (57.5°) between the carbazole and HDTBT units due to steric hindrance of the hexyl substituents on the thienyl groups.[26] In the cathodic scan, onset potentials of the reduction wave were similar, in the range of −0.79−0.88 V. This result indicated that the LUMO was essentially dominated by the acceptor unit, benzothiadiazole, which further explains why the dihedral angle between BT and the thienyl group was less than 5° in all copolymers, as mentioned in the discussion of the computational study.

The electrochemical bandgap ($\Delta E_{e,film}$) in the films was calculated from the voltage difference between the onset potentials of oxidation and reduction. The trend in the copolymer bandgaps followed the trend observed for the optical bandgaps ($\Delta E_{e,film}$). $\Delta E_{e,film}$ for P(3,6C-DTBT) was 1.71 eV, which was 0.18 eV lower than that of P(2,7C-DTBT). This provided further evidence for strong intramolecular CT and robust short-range conjugation in P(3,6C-DTBT), as observed in the absorption measurements. In contrast, $\Delta E_{e,film}$ for copolymers with larger dihedral angles increased to 2.16 eV, demonstrating that severe steric hindrance from the hexyl substituents on the thienyl groups disrupted conjugation between the carbazole and HDTBT.

Fluorescence Properties. Photoluminescence (PL) measurements are one of the best methods for estimating the extent of π-conjugation in the excited state. It may be applied not only toward intramolecular interactions but also toward intermolecular interactions.[51] Figure 7a shows the PL spectra of the copolymers in chloroform (10^{-5} M). The emission maxima (λ_{max}) appeared in the long wavelength region (500−900 nm) as single peaks upon excitation at the absorption maxima. The PL spectra were probably due to intermolecular CT from the carbazole units to the electron-deficient DTBT or HDTBT.[35,40] The PL peaks of the substituted copolymers P(2,7C-HDTBT) and P(3,6C-HDTBT) were shifted to shorter wavelengths relative to the corresponding unsubstituted copolymers, P(2,7C-DTBT) and P(3,6C-DTBT), respectively, due to a decrease in population of the quinoidal electronic configuration[52] as a result of twisting of the dihedral angle. Interestingly, emission of P(3,6C-DTBT), which included conjugation breaks, appeared at longer wavelengths compared with P(2,7C-DTBT). The solvatochromic effect was investigated as a possible explanation for the results, as shown in Figure 8 (see the Supporting Information for P(2,7C-DTBT) and P(2,7C-HDTBT), Figure S4). As the solvent polarity increased, PL peaks shifted to the red. The red shifts in the PL spectra were probably due to interactions between the strongly bound polarized excitons and the polar solvent, indicating that the solvent relaxed the excited state of the copolymers. P(3,6C-DTBT) exhibited a slightly stronger solvent dependence than P(2,7C-DTBT), supporting the extra stabilization of excitons between the isolated conjugation breaks. This result suggests an explanation for the 24 nm red shift in the emission of P(3,6C-DTBT) in thin films in comparison with that in chloroform (Figure 7b): the distance between polarized excitons in the film may be very close.

To investigate the competition between intramolecular and intermolecular charge transfer interactions, the emission spectra

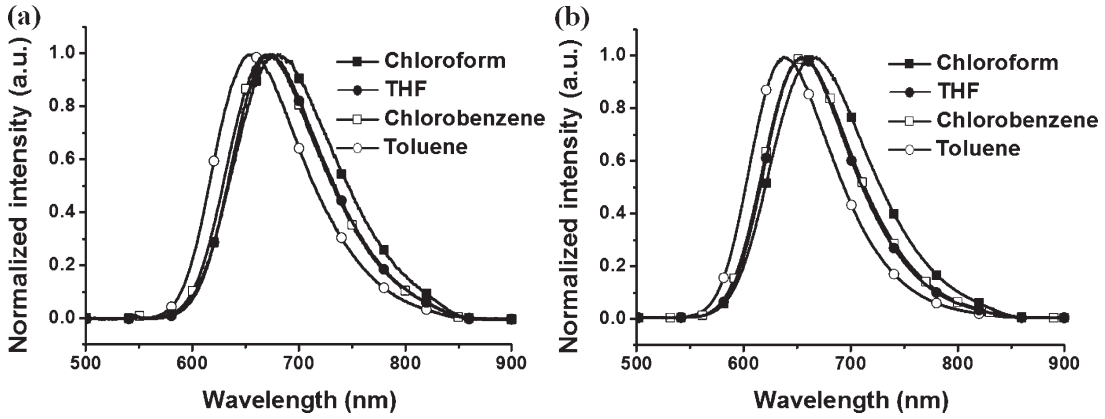

Figure 8. Normalized PL spectra: (a) P(3,6C-DTBT) (b) P(3,6C-HDTBT) in chloroform (■), THF (●), chlorobenzene (□), and toluene (○). The absorption maxima in short wavelength region, for each sample, were chosen for excitation.

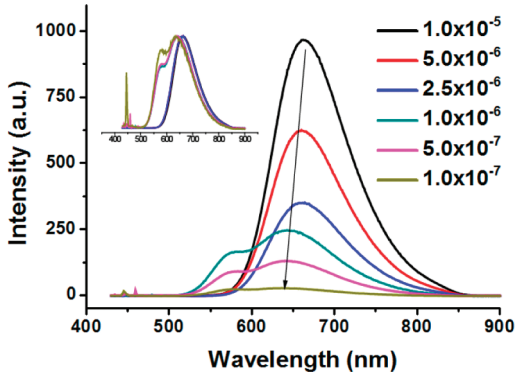

Figure 9. PL spectra of P(2,7C-DTBT) in various concentrations (normalized PL spectra of the polymer were inserted).

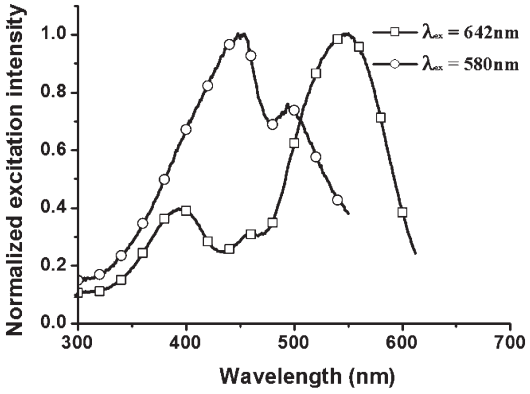

Figure 10. Normalized excitation spectra of P(2,7C-DTBT) excited at λ_{ex} = 642 nm (□) and and 580 nm (○) in chloroform at a concentration of 1×10^{-7} M.

of the copolymers were recorded at various concentrations in chloroform. As the P(2,7C-DTBT) solution was diluted, the emission intensities decreased proportional to the concentration and the peak shifted toward the blue. Interestingly, a distinctive hump near 580 nm appeared below 1×10^{-6} M, as shown in Figure 9. Under such dilute conditions, the distance between molecules was too large to permit the transfer of energy, and intramolecular CT was favored. Therefore, the new emission band at 580 nm may have originated from intramolecular CT. An

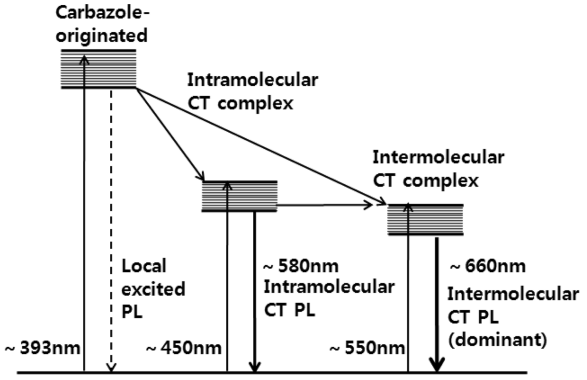

Figure 11. Jablonski diagram presenting the possible excitation and relaxation pathways for P(2,7C-DTBT).

analogous hump was observed in the spectrum of P(3,6C-DTBT), but at much lower concentrations (below 1×10^{-7} M). P(2,7C-HDTBT) and P(3,6C-HDTBT) did not exhibit any additional emission bands, even at concentrations of 1×10^{-9} M (see the Supporting Information, Figure S5). The conjugation length of P(2,7C-DTBT) was longer than that of the other copolymers, but particularly longer than the conjugation lengths of P(2,7C-HDTBT) and P(3,6C-HDTBT). Therefore, we conclude that intramolecular CT was more favorable in copolymers with longer conjugation lengths.

The appearance of the hump was examined more closely as a function of the copolymer structure. To do so, the excitation spectra were monitored at the emission maxima. Figure 10 shows the excitation spectra of P(2,7C-DTBT) monitored at 642 nm, which is the PL maximum of the P(2,7C-DTBT) solution at a concentration of 1×10^{-7} M. Three distinctive excitation peaks were located at 550, 450, and 390 nm. Among them, the 550 and 390 nm peaks could be assigned to excitations of the carbazole and DTBT units, respectively, by comparison with the UV−vis absorption spectra (see Figure 4). The peak at 450 nm was identified by measuring the excitation spectra at the emission wavelength of 580 nm (the hump peak) at low concentrations. A strong excitation peak at 450 nm was obtained. This result strongly suggested that the hump appearing at 580 nm (Figure 9) in dilute solutions originated from intramolecular CT. On the basis of this result, a Jablonski diagram for the electronic state of P(2,7C-DTBT) was constructed, as shown in Figure 11.

dx.doi.org/10.1021/ma102467w |*Macromolecules* 2011, 44, 1909–1919

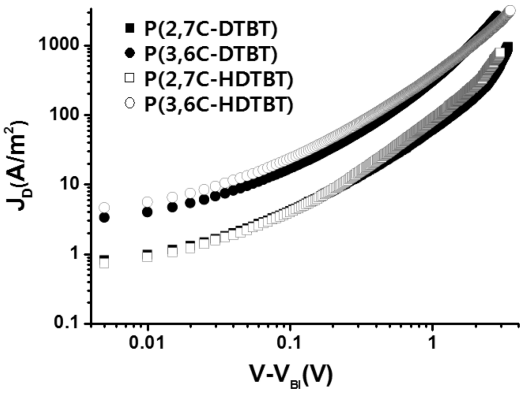

Figure 12. $J-V$ characteristics of P(2,7C-DTBT) (■), P(3,6C-DTBT) (●), P(2,7C-HDTBT) (□), and P(3,6C-HDTBT) (○) under dark conditions (ITO/PEDOT:PSS (36 nm)/active layer (~50 nm)/Pd).

Charge Carrier Mobility Properties. The electronic characteristics of the copolymers were investigated with the goal of identifying materials with potential for application in organic electronics. We extracted and calculated the hole mobilities of the copolymers from space charge limited current (SCLC) measurements in hole-only devices.[53,54] The dark current characteristics of ITO/PEDOT:PSS (36 nm)/polymer (~50 nm)/Pd devices clearly exhibited Ohmic behavior at low voltages and trap-free SCLC behavior at high voltages (Figure 12). The SCLC characteristics of the trap-free region were modeled using the Mott–Gurney square law: $J = (9/8)\varepsilon\mu(V^2/L^3)$, where J is the current density through the device, V is the voltage drop across the device, L is the thickness of the polymer film, ε is the static dielectric constant of the medium, and μ is the carrier mobility.[55] The calculated hole mobilities of the copolymers are summarized in Table 3.

Interestingly, the 3,6-carbazole-based polymers, P(3,6C-DTBT) and P(3,6C-HDTBT), exhibited an order of magnitude higher mobility than the 2,7-carbazole-based polymers, P(2,7C-DTBT) and P(2,7C-HDTBT) (1.2×10^{-5} cm^2 V^{-1} s^{-1}, compared with $(3.0-3.2) \times 10^{-6}$ cm^2 V^{-1} s^{-1}). An external voltage in hole-only devices produced cations, which acted as charge carriers on the carbazole unit. The nitrogen atom on the carbazole unit of P(2,7C-DTBT) was in the *m*-position with respect to the conjugated backbone and was linked to the thienylbenzothiadiazole. Therefore, intramolecular charge delocalization was not allowed, and conjugation was tied to a single repeating unit.[10] In contrast, delocalization across the 3,6-carbazole units of P(3,6C-DTBT) and P(3,6C-HDTBT) could be expanded, at least within conjugation breaks.[56] The mobilities of the unsubstituted copolymers and substituted copolymers were nearly identical. The mobility of the low molecular weight P(3,6C-DTBT) was comparable to that of P(3,6C-HDTBT). These observations suggest that a structural dependence of the charge mobility was dominant, at least in these copolymers.

■ CONCLUSIONS

A series of well-defined, carbazole-based alternating copolymers with dithienylbenzothiadiazole (DTBT and HDTBT) was prepared in good yields using a Suzuki cross-coupling reaction. The thermal, optical, electrochemical, and electronic properties of the copolymers were fully characterized. The copolymers exhibited remarkable thermal stability up to 420 °C, as revealed by TGA. The position of the carbazole linkage and the presence of steric hindrance between the donor and acceptor were found to dramatically influence the electrochemical and electronic properties of the copolymers. Intramolecular CT was observed from carbazole to DTBT through the backbone, even in the ground state of P(2,7C-DTBT), due to the long conjugation length. Intramolecular CT resulted in a large absorption coefficient. Conjugation breaks in the middle of the carbazole units were present in P(3,6C-DTBT) and resulted in robust coplanarity between the carbazole and the DTBT, thereby lowering the oxidation potential and increasing the rigidity of the chain. In addition, strong intramolecular CT in P(3,6C-DTBT) occurred in the ground state within isolated conjugation breaks, resulting in optical and chemical bands that were similar to those of P(2,7C-DTBT). Excitons located between isolated conjugation breaks in P(3,6C-DTBT) were highly stable and emitted the longest wavelength PL emission. Introduction of alkyl substituents at the 4-position of the thienyl moiety in DTBT provided significant steric hindrance, thereby increasing the dihedral angel between the carbazole and HDTBT. Therefore, steric hindrance perturbed the backbone conjugation more than the conjugation breaks and increased the solubility of high molecular weight P(3,6C-HDTBT). The charge carrier mobilities of the copolymers depended only on the position of the nitrogen atom. The hole mobilities of 3,6-carbazole-based copolymers were an order of magnitude greater than those of 2,7-carbazole-based copolymers. These systematic studies clarify the parameters by which D-π-A copolymers may be fine-tuned for a particular purpose. This work additionally provides a better understanding of the relationship between structural and optical or electronic properties in copolymers to assist in a variety of optoelectronic applications.

■ ASSOCIATED CONTENT

Ⓢ Supporting Information. TGA thermograms, UV–vis absorption and PL spectra in various solvents, and energy maps of dihedral angles and their energy for optimized geometry of all the copolymers. This material is available free of charge via Internet at http://pubs.acs.org.

■ AUTHOR INFORMATION

Corresponding Author
*E-mail taihopark@postech.ac.kr; Tel +82-54-279-2394.

■ ACKNOWLEDGMENT

This work was supported by a grant (M2009010025) from the Fundamental R&D Program for Core Technology of Materials funded by the MKE, by the Midcareer Researcher Program and the Basic Science Research Program through a National Research Foundation of Korea (NRF) grant funded by the MEST (No. 2009-0079879, No. 2009-0093462), and by the second stage of a BK21 (Brain Korea 21) grant.

■ REFERENCES

(1) (a) Burroughes, J. H.; Bradley, D. D. C.; Brown, A. R.; Marks, R.; Mackay, N. K.; Friend, R. H.; Holmes, A. B. *Nature* **1990**, *347*, 539–541. (b) Friend, R. H.; Gymer, R. W.; Holmes, A. B.; Burroughes, J. H.; Marks, R. N.; Taliani, C.; Bradley, D. D. C.; Santos, D. A.; Brédas, J. L.; Lögdlund, M.; Salaneck, W. R. *Nature* **1999**, *397*, 121–128. (c) Kraft, A.;

Grimsdale, A. C.; Holmes, A. B. *Angew. Chem., Int. Ed.* **1998**, *37*, 402–428.
(2) (a) Dimitrakopoulos, C. D.; Kymissis, J.; Purushothaman, S.; Neumayer, D. A.; Duncombe, P. R.; Laibowitz, R. B. *Adv. Mater.* **1999**, *11*, 1372–1375. (b) Horowitz, G.; Hajlaoui, P.; Delannoy, P. *J. Phys. III* **1995**, *5*, 355–372. (c) Horowitz, G.; Hajlaoui, R.; Fichou, D.; El Kassmi, A. *J. Appl. Phys.* **1999**, *85*, 3202–3206.
(3) (a) Ma, W.; Yang, C.; Gong, X.; Lee, K.; Heeger, A. J. *Adv. Funct. Mater.* **2005**, *15*, 1617–1622. (b) Reyes-Reyes, M.; Kim, K.; Carroll, D. L. *Appl. Phys. Lett.* **2005**, *87*, 083506. (c) Li, G.; Shrotriya, V.; Huang, J.; Yao, Y.; Moriarty, T.; Emery, K.; Yang, Y. *Nature Mater.* **2005**, *4*, 864–868.
(4) Morin, J.-F.; Leclerc, M.; Adés, D.; Siove, A. *Macromol. Rapid Commun.* **2005**, *26*, 761–778.
(5) Iraqi, A.; Wataru, I. *Chem. Mater.* **2004**, *16*, 442–448.
(6) Pickup, D. F.; Yi, H.; Kun, H.; Iraqi, A.; Stevenson, M.; Lidzey, D. G. *Thin Solid Films* **2009**, *517*, 2840–2844.
(7) Morin, J.-F.; Leclerc, M. *Macromolecules* **2002**, *35*, 8413–8417.
(8) Lai, M.-H.; Tsai, J.-H.; Chueh, C.-C.; Wang, C.-F.; Chen, W.-C. *Macromol. Chem. Phys.* **2010**, *211*, 2017–2025.
(9) Dierschke, F.; Grimsdale, A. C.; Müllen, K. *Synthesis* **2003**, *16*, 2470.
(10) Zotti, G.; Schiavon, G.; Zecchin, S.; Morin, J.-F.; Leclerc, M. *Macromolecules* **2002**, *35*, 2122.
(11) Tirapattur, S.; Belletête, M.; Drolet, N.; Leclerc, M.; Durocher, G. *Chem. Phys. Lett.* **2003**, *370*, 799–804.
(12) Li, J.; Grimsdale, A. C. *Chem. Soc. Rev.* **2010**, *39*, 2399–2410.
(13) Park, J. S.; Song, M.; Jin, S.-H.; Lee, J. W.; Lee, C. W.; Gal, Y.-S. *Macromol. Chem. Phys.* **2009**, *210*, 1572–1578.
(14) Morin, J.-F.; Beaupré, L. M.; Lévesque, I.; D'Iorio, M. *Appl. Phys. Lett.* **2002**, *80*, 341–343.
(15) Witker, D.; Reynolds, J. R. *Macromolecules* **2005**, *38*, 7636–7644.
(16) Jin, S.-H.; Kim, W.-H.; Song, I.-S.; Kwon, S.-K.; Lee, K.-S.; Han, E.-M. *Thin Solid Films* **2000**, *363*, 255–258.
(17) Song, S.-Y.; Jang, M. S.; Shim, H.-K. *Macromolecules* **1999**, *32*, 1482–1487.
(18) Sotzing, G. A.; Reddinger, J. L.; Katritzky, A. R.; Soloducho, J.; Musgrave, R.; Reynolds, J. R. *Chem. Mater.* **1997**, *9*, 1578–1587.
(19) Mortimer, R. J.; Dyer, A. L.; Reynolds, J. R. *Display* **2006**, *27*, 2–18.
(20) Gaupp, C. L.; Reynolds, J. R. *Macromolecules* **2003**, *36*, 6305–6315.
(21) Iraqi, A.; Pickup, D. F.; Yi, H. *Chem. Mater.* **2006**, *18*, 1007–1015.
(22) Hunag, J.; Niu, Y.; Yang, W.; Mo, Y.; Yuan, M.; Cao, Y. *Macromolecules* **2002**, *35*, 6080–6082.
(23) Du, J.; Fang, Q.; Chen, X.; Ren, S.; Cao, A.; Xu, B. *Polymer* **2005**, *46*, 11927–11933.
(24) Wang, Y.; Hou, L.; Yang, K.; Chen, J.; Wang, F.; Cao, Y. *Macromol. Chem. Phys.* **2005**, *206*, 2190–2198.
(25) Li, Y.; Ding, J.; Day, M.; Tao, Y.; Lu, J.; D'iorio, M. *Chem. Mater.* **2004**, *16*, 2165.
(26) Song, S.; Jin, Y.; Kim, S. H.; Moon, J.; Kim, K.; Kim, J. Y.; Park, S. H.; Lee, K.; Suh, H. *Macromolecules* **2008**, *41*, 7296–7305.
(27) Zhou, H.; Yang, L.; Xiao, S.; Liu, S.; You, W. *Macromolecules* **2010**, *43*, 811–820.
(28) Wang, E.; Wang, M.; Wang, L.; Duan, C.; Zhang, J.; Cai, W.; He, C.; Wu, H.; Cao, Y. *Macromolecules* **2009**, *42*, 4410–4415.
(29) Qin, R.; Li, W.; Li, C.; Du, C.; Veit, C.; Schleiermacher, H.-F.; Andersson, M.; Bo, Z.; Liu, Z.; Inganäs, O.; Wuerfel, U.; Zhang, F. *J. Am. Chem. Soc.* **2009**, *131*, 14612–14613.
(30) Shin, C.-K.; Lee, H. *Synth. Met.* **2004**, *80*, 271–277.
(31) Zhang, Y.; Tajima, K.; Hirota, K.; Hashimoto, K. *J. Am. Chem. Soc.* **2008**, *130*, 7812–7813.
(32) Blouin, N.; Michaud, A.; Leclerc, M. *Adv. Mater.* **2007**, *19*, 2295–2300.
(33) Hou, Q.; Xu, Y.; Yang, W.; Yuan, M.; Peng, J.; Cao, Y. *J. Mater. Chem.* **2002**, *12*, 2887–2892.
(34) Hou, Q.; Zhou, Q.; Zhang, Y.; Yang, W.; Yang, R.; Cao, Y. *Macromolecules* **2004**, *37*, 6299–6305.
(35) Romero, D. B.; Schaer, M.; Leclerc, M.; Adès, D. J.; Siove, A.; Zuppiroli, L. *Synth. Met.* **1996**, *80*, 271–277.
(36) Miyaura, N.; Suzuki, A. *Chem. Rev.* **1995**, *95*, 2457–2483.
(37) Blouin, N.; Michaud, A.; Gendron, D.; Wakim, S.; Blair, E.; Neagu-Plesu, R.; Belletête, M.; Durocher, G.; Tao, Y.; Leclerc, M. *J. Am. Chem. Soc.* **2008**, *130*, 732–742.
(38) Fu, Y.; Bo, Z. *Macromol. Rapid Commun.* **2005**, *26*, 1704–1710.
(39) Huang, J.; Xu, Y.; Hou, Q.; Yang, W.; Yuan, M.; Cao, Y. *Macromol. Rapid Commun.* **2002**, *23*, 709–712.
(40) Huang, J.; Xu, Y.; Hou, Q.; Yang, W.; Yuan, M.; Cao, Y. *Macromol. Rapid Commun.* **2002**, *23*, 709–712.
(41) Zhang, Z.-B.; Fujiki, M.; Tang, H-. Z.; Motonaga, M.; Torimitsu, K. *Macromolecules* **2002**, *35*, 1988–1990.
(42) Iraqi, A.; Wataru, I. *J. Polym. Sci., Part A: Polym. Chem.* **2004**, *42*, 6041–6051.
(43) Jayakannan, M.; Hal, P. A. V.; Janssen, R. A. J. *J. Polym. Sci., Part A: Polym. Chem* **2002**, *40*, 251–261.
(44) Jenekhe, S. A.; Lu, L.; Alam, M. M. *Macromolecules* **2001**, *34*, 7315–7324.
(45) Panthi, K.; Adhikari, R. M.; Kinstle, T. H. *J. Phys. Chem. A* **2010**, *114*, 4550–4557.
(46) Becke, A. D. *J. Chem. Phys.* **1993**, *98*, 5648–5652.
(47) Lee, C. T.; Yang, W. T.; Parr, R. G. *Phys. Rev. B* **1988**, *37*, 785–789.
(48) Bredas, J. L.; Silbey, R.; Boudreaux, D. S.; Chance, R. R. *J. Am. Chem. Soc.* **1983**, *105*, 6555–6559.
(49) Ambrose, J. F.; Carpenter, L. L.; Nelson, R. F. *J. Electrochem. Soc.* **1975**, *122*, 876–894.
(50) Ambrose, J. F.; Nelson, R. F. *J. Electrochem. Soc.* **1968**, *115*, 1159–1164.
(51) Sixl, H. *Mol. Cryst. Liq. Cryst.* **1986**, *134*, 65–88.
(52) Du, J.; Xu, E.; Zhong, H.; Yu, F.; Liu, C.; Wu, H.; Zeng, D.; Ren, S.; Sun, J.; Liu, Y.; Cao, A.; Fang, Q. *J. Polym. Sci., Part A: Polym. Chem* **2008**, *46*, 1376–1387.
(53) Mihailetchi., V. D.; Xie, H.; de Boer, B.; Koster, L. J. A.; Blom, P. W. M. *Adv. Funct. Mater.* **2004**, *14*, 865–870.
(54) Zhao, Y.; Xie, Z.; Qu, Y.; Geng, Y.; Wang, L. *Appl. Phys. Lett.* **2007**, *90*, 043504–043506.
(55) Park, J. H.; Kim, J. S.; Lee, J. H.; Lee, W. H.; Cho, K. *J. Phys. Chem. C* **2009**, *113*, 17579–17584.
(56) Siove, A.; Adès, D.; Ngbilo, E.; Chevrot, C. *Synth. Met.* **1990**, *38*, 331–340.